Exciton-photon interaction in low-dimensional semiconductor microcavities

A. I. Tartakovskiĭ*) and V. D. Kulakovskiĭ

Institute of Solid-State Physics, Russian Academy of Sciences, 142432 Chernogolovka, Moscow Region, Russia

Yu. I. Koval' and T. B. Borzenko

Institute of Problems in the Technology of Microelectronics and High-Purity Materials, Russian Academy of Sciences, 142432 Chernogolovka, Moscow Region, Russia

A. Forchel and J. P. Reithmaier†)

Technische Physik, Universität Würzburg, D 97074 Würzburg, Germany
(Submitted 5 January 1998)
Zh. Éksp. Teor. Fiz. **114**, 1329–1345 (October 1998)

The structure of the photon states and dispersion of cavity polaritons in semiconductor microcavities with two-dimensional optical confinement (photon wires), fabricated from planar Bragg structures with a quantum well in the active layer, are investigated by measuring the angular dependence of the photoluminescence spectra. The size quantization of light due to the wavelength-commensurate lateral dimension of the cavity causes additional photon modes to appear. The dispersion of polaritons in photon wires is found to agree qualitatively with the prediction for wires having an ideal quantum well, for which the spectrum is formed by pairwise interaction between exciton and photon modes of like spatial symmetry. The weak influence of the exciton symmetry-breaking random potential in the quantum well indicates a mechanism of polariton production through light-induced collective exciton states. This phenomenon is possible because the light wavelength is large in comparison with the exciton radius and the dephasing time of the collective exciton state is long. © *1998 American Institute of Physics.* [S1063-7761(98)01210-4]

1. INTRODUCTION

Semiconductor microcavities with imbedded quantum wells are currently stimulating a growing interest among researchers. They are intersting in connection with the feasibility of monitoring and investigating the modification of exciton properties as a result of the mixing of exciton states with cavity optical modes. In particular, exciton-photon interaction leads to Rabi splitting and modification of the dispersion of exciton and photon modes.[1–5] The bulk of the experimental papers report the interaction of light and excitons in cavities that imbed one or more quantum wells situated at antinodes of the optical electromagnetic field in an active layer of thickness λ or $(3/2)\lambda$ contained between two Bragg mirrors.[6–8] This geometry can be regarded as two-dimensional (2D) both for excitons in a well and for light in a Fabry–Perot cavity. In a planar microcavity optical momentum is not conserved in the direction perpendicular to the planes of the mirrors, whereas in a plane parallel to the mirrors the quasimomentum is a ''good'' quantum number, and the photon mode has a completely defined dependence of the energy E on k. This dependence can be measured by recording the reflection, transmission, or luminescence signal at various angles ϕ relative to the plane of the sample.[7] The planar quasimomentum k is related to the light momentum in vacuum q by the equation

$$k = q \sin \phi. \tag{1}$$

Here the dispersion of light in the empty microcavity is described by the expression[5,7]

$$E_k = \sqrt{E_v^2 + \alpha k^2}, \tag{2}$$

where E_v is the energy of the vertical cavity mode, and the coefficient α depends on the effective dielectric permittivity. In a microcavity containing quantum wells the energy of the photon and exciton modes is modified by the interaction of excitons in the wells with light. In the presence of strong exciton–photon coupling the exciton and photon dispersion branches are repulsive and can be described on the basis of the polariton model. The dispersion of a cavity polariton was first measured in Ref. 7 from an analysis of the angular dependence of the energies of the luminescence peaks at low excitation densities.

Papers have also been published very recently, describing investigations of three-dimensionally (3D) optically confined semiconductor microcavities, i.e., photon dots.[9,10] In these structures, with dimensions of the order of a few micrometers, light has been quantized in one dimension by means of Bragg mirrors and in the other two dimensions by a large difference in the refractive indices at the semiconductor–vacuum boundary. The localization of light in such structures produces a discrete photon spectrum, where the energy distance between modes increases as the size of the dot decreases. The dispersion of photon modes does not occur in such a cavity.

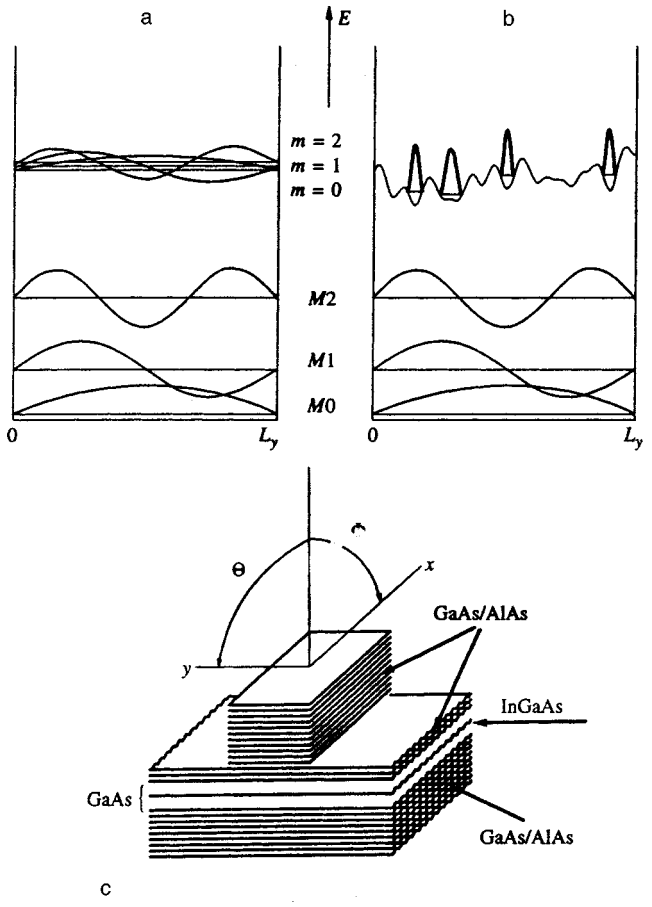

FIG. 1. a) Diagram of the exciton and photon states in photon wires with an ideal quantum well; b) the same with quantum-well localization of excitons by a random potential; c) schematic view of the sample, showing the planes in which the angles Φ and Θ are plotted.

In this paper we report an investigation of the dispersion of polaritons and the role of exciton–photon interaction in microcavities with 2D light quantization. Such cavities are aptly called photon wires. In photon wires 3D light confinement leads to the additional quantization of cavity photon states over and above the quantization in planar cavities, but in contrast with photon dots, all modes exhibit one-dimensional dispersion along the axis of the wire (x axis).

A diagram of the size-quantization levels in a microcavity of width L_y containing an ideal quantum well is shown in Fig. 1a. To simplify the diagram, only three exciton quantization levels ($m=0,1,2$) and three photon states ($M0, M1, M2$) situated below the exciton energy are shown in the figure. Under conditions such that the light wavelength is commensurate with the transverse dimensions of the cavity, the photon quantization energies attain several millielectron volts; on the other hand, owing to the large translational mass of the exciton, the energies of exciton states with different numbers m ($m=n-1$, where n is the number of the size-quantization level) differ only very slightly. Figure 1a also shows the exciton and photon wave functions corresponding to levels with different quantum numbers. The wave functions of excitons and photons with identical m have the same symmetry.

Exciton–photon interaction in one-dimensional microcavities with an ideal quantum well will necessarily lead to the mixing of photon and exciton states having the same spatial symmetry. This means that as the wave vector k_x increases, all photon modes whose energy at zero quasimomentum was lower than the exciton energy must make an anticrossing with an exciton mode of the same symmetry.[1)] For the case illustrated in Fig. 1a strong exciton–photon coupling results in the formation of three lower (Mm_L) and three upper (Mm_U) polariton modes.

In real quantum wells the localization of excitons by a random potential breaks the symmetry of the exciton states (Fig. 1b). The influence of a random potential on the formation and radiative properties of polaritons in planar microcavities has been a topic of debate up to this point.[11–13,15] In a system with broken spatial symmetry of the exciton states a light wave interacts with all excitons. In this case the properties of the polariton states depend on the dephasing time.[16] In photon wires, as opposed to planar microcavities, there are optical modes with different spatial symmetries. For this reason the investigation of polariton phenomena in low-dimensional microcavities offers deeper insight into the mechanism underlying the interaction of light with excitons in a system with disorder. The experimental results obtained in the present study suggest that the dispersion of polaritons in the investigated one-dimensional microcavities coincides with the expected dispersion for a resonator having an ideal quantum well. The reasons for the weak influence of exciton localization in quantum wells will be discussed below.

The article is organized as follows: In Sec. 2 we describe the method of preparation and the structure of the photon wires, along with the experimental technique; in Sec. 3 we discuss the structure, measured at high excitation density, of the optical states in photon wires in the presence of weak exciton–photon interaction; in Sec. 4 we describe the variation of the exciton–photon interaction as the density of excitons varies, along with the transition from the quantization of photon states to the quantization of polariton states; in Sec. 5 we discuss the dispersion of polaritons in photon wires in the presence of strong exciton–photon coupling, as determined experimentally at low excitation densities.

2. THE SAMPLE AND EXPERIMENTAL TECHNIQUE

For the measurements we used a microcavity structure grown by molecular-beam epitaxy. The active element of the microcavity comprises an $In_{0.14}Ga_{0.86}As$ quantum well of width 70 Å contained in a GaAs λ-layer between two Bragg mirrors. The active GaAs layer is wedge-shaped, making it possible (by exciting luminescence at different points of the sample) to vary the energy distance between the Fabry–Perot mode and the exciton level. The Bragg mirrors, having better than 99% reflectivity, consist of 17 and 21 AlAs/GaAs pairs (above and below the active layer, respectively), where each layer has a width equal to $\lambda/4$. Arrays of photon wires having widths from 4.2 μm to 6.2 μm were prepared by electron-beam lithography and ion-beam etching. A polymethyl methacrylate PMMA 950 K electronic resist of thickness 1.5 μm was deposited on the sample, and windows in the form of wires were opened in the resist by electron-beam

lithography. Next, an Al layer of thickness 1 μm was sprayed onto the entire sample, and explosion lithography was applied. The stenciled Al pattern then served as a mask for ion-beam etching. Etching was performed with 500-eV Ar ions at a current density of 0.1 mA/cm^2. Oblique low-temperature etching is known to have the potential benefit of reducing radiation damage to structures.[14] During etching, therefore, the sample was tilted at a 75° angle relative to the direction of the ion beam and was precisely oriented in such a way as to align the direction of incidence of the ions with the wires. The sample was kept at a temperature of 77 K during etching. Only the upper mirror of the microcavity etched, leaving two or three pairs of AlAs/GaAs layers between the untouched surfaces of the photon wires. A diagram of the sample is shown in Fig. 1c. Also shown in the figure are the planes in which were measured the angles Θ and Φ used in our description of the experimental results.

The dispersion of cavity polaritons was investigated by analyzing the angular dependence of the luminescence spectra. The sample was placed in an optical cryostat in helium vapor at a temperature $T=5$ K. Luminescence was excited by a HeNe or Ar^+ laser and was recorded by means of a 0.5 m monochromator and a nitrogen-cooled CCD camera. A laser beam modulator was used to avoid overheating of the sample at high excitation power.

3. PHOTON MODES IN A ONE-DIMENSIONAL MICROCAVITY

The quantization of light in a one-dimensional cavity causes a photon mode to split into states that have dispersion only in the direction of the axis of the wire (x axis). The photon mode energy Mm can be described by the expression[9]

$$E_m(k_x)=\sqrt{E_v^2+\frac{\hbar^2c^2}{\varepsilon_{\text{eff}}}\left[k_x^2+\frac{(m+1)^2\pi^2}{L_y^2}\right]}. \tag{3}$$

Here $m=0,1,\ldots$, L_y is the width of the wire, and ε_{eff} is the effective dielectric constant.[9] Calculations also show that the intensity maxima of the excited states of the one-dimensional photon system are detected at nonzero angles Θ because of the different symmetries of the field distribution in the cavity interior for different mode orders. In addition, it follows from these calculations that for $\Theta=0°$ mode $M0$ has an intensity maximum, and mode $M2$ has a local maximum.[15]

It has been shown[8] that for high excitation densities the mixing of exciton and photon modes in the cavity tends to be suppressed and does not influence the type of dispersion of the photon modes when the carrier density in the quantum well corresponds to the onset of an electron–hole plasma. Consequently, the energies and dispersion of the cavity photon modes for $k=0$ can be measured by analyzing the emission spectra recorded in the presence of a sufficiently high excitation density.

Figure 2 shows luminescence spectra recorded for wires of width 4.2 μm at $\Phi=0°$ and at various detection angles Θ for a high excitation density ($P=1600$ W/cm^2). For this excitation density the carrier density created in the quantum well is greater than 10^{11} cm^{-2}. At this density screening plays a significant part, while exciton effects and, accordingly, exciton–photon interaction tends to be suppressed. In Fig. 2 photon modes with different quantum numbers are seen in all the spectra as strong, narrow lines. The energy positions of the photon modes are indicated by vertical arrows. The wide line with a maximum in the vicinity of 1.413 eV, labeled $e-h$, corresponds to a recombination peak of a dense exciton system. As expected, the quantization of the system in a direction perpendicular to the axis of the wire renders the energies of the photon modes independent of the angle Θ. At $\Theta=0°$ only odd mode orders ($M1, M3, \ldots$) are strictly forbidden. Consequently, in addition to the ground photon state $M0$, a feature corresponding to mode $M2$ is also visible in the luminescence spectrum at $\Theta=0°$. As Θ increases, states corresponding to mode orders $m>0$ successively appear and disappear (as the angle is further increased) in the luminescence spectra. It is evident from the figure that optical modes up to $M4$ are clearly visible in the spectra for $\Theta\leqslant 23°$.

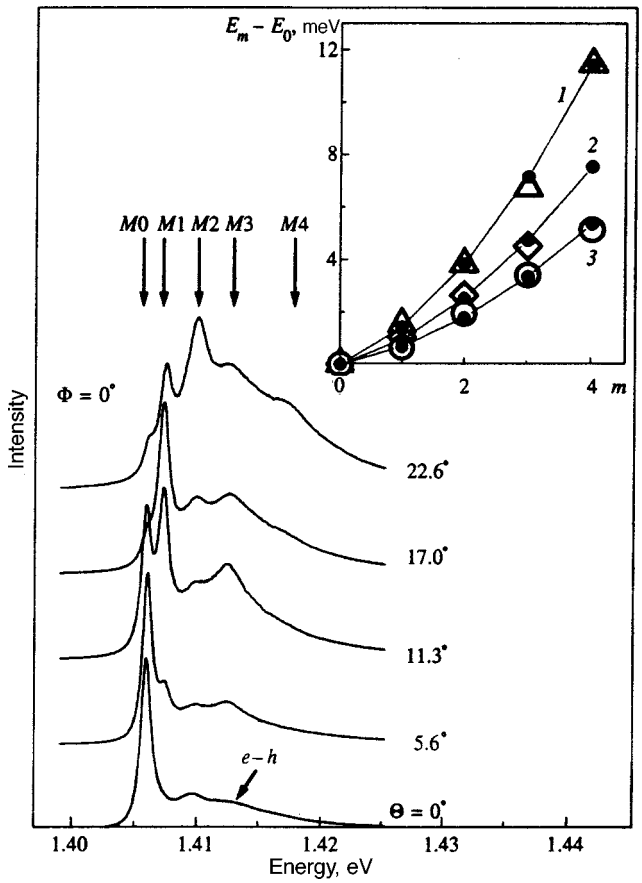

FIG. 2. Photoluminescence spectra for wires with $L_y=4.2$ μm, recorded for a high excitation density at $\Phi=0°$ and various angles Θ. The vertical arrows indicate the positions of modes with different quantum numbers m. The electron–hole recombination peak is labeled e-h. Inset: splitting $\Delta E_{m0}=E_m-E_0$ as a function of the mode order m for wires of various widths. The triangles correspond to splitting for a wire of width 4.2 μm, the diamonds correspond to 5.2 μm, and the circles correspond to 6.2 μm. Dark symbols, which are joined by smooth curves to aid visualization, represent the results of calculations according to Eq. (3) at $k_x=0$. Effective wire width d_{eff} used for curve fitting: *1)* 5.2 μm; *2)* 6.4 μm; *3)* 7.6 μm.

The inset to Fig. 2 shows the splittings $\Delta E_{m0}=E_m-E_0$ between optical modes, measured for photon wires of various widths. The triangles in the inset correspond to split-

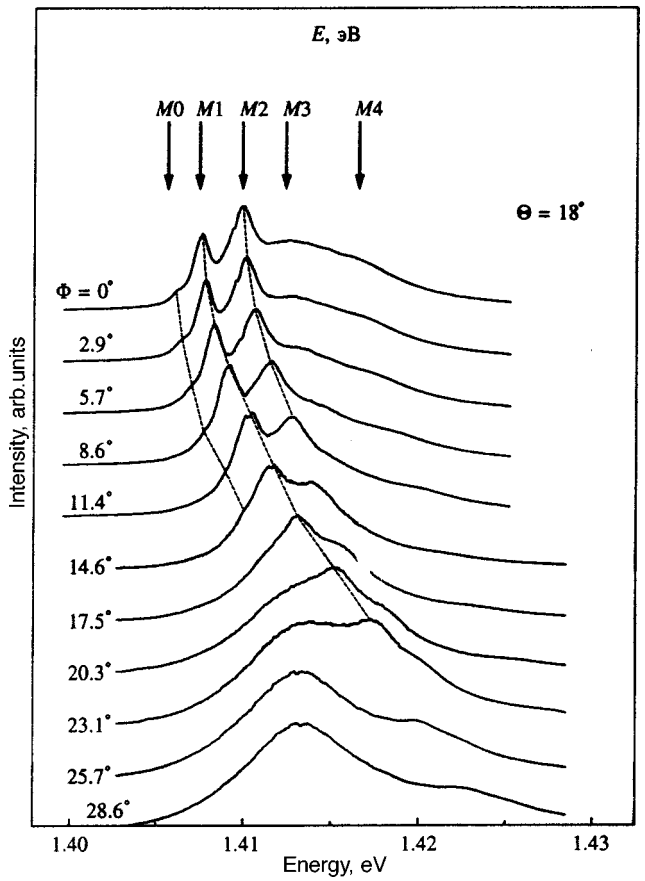

FIG. 3. Photoluminescence spectra for wires with $L_y = 4.2\ \mu$m, recorded for a high excitation density at $\Theta = 18°$ and various angles Φ. The vertical arrows indicate the mode positions for $\Phi = 0°$. The dashed curves represent the positions of modes $M0$, $M1$, and $M2$, as functions of the angle Φ.

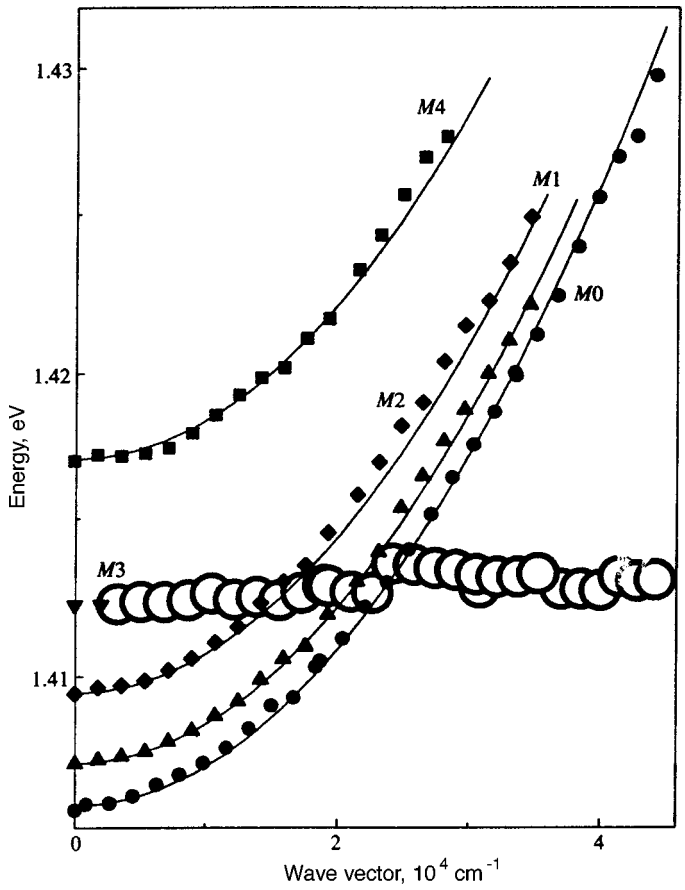

FIG. 4. Dispersion of photon modes of a wire with $L_y = 4.2\ \mu$m for a high excitation density. Dark symbols represent the measured photon mode positions. The light circles represent the position of the electron–hole recombination peak. The solid curves are calculated from Eq. (3).

tings for a wire of width 4.2 μm, the diamonds correspond to 5.2 μm, and the circles correspond to 6.2 μm. It is evident from the figure that the splitting of the photon modes decreases as the width of the wire increases. We use Eq. (3) with $k_x = 0$ to describe the splitting between optical modes. The role of the fitting parameter in this case is taken by the effective width of the wire d_{eff}. In the inset to Fig. 2 the calculations of ΔE_{m0} according to (3) are represented by dark symbols joined by solid lines. The value of d_{eff} used in the calculations is given for each curve. It is evident from the figure that the behavior of the experimentally measured dependence of the splitting on the width of the wire is qualitatively consistent with the calculations according to (3). However, the values of d_{eff} are found to be greater than the true widths of the photon wires. We identify this discrepancy primarily with the fact that the Bragg mirrors left unetched to the very end in the regions between the photon wires permit light to penetrate beyond the limits of the wires, and this process, in turn, causes the effective width of the cavity to increase.

In photon wires light is not quantized in the direction of the wire axis. The energy of the photon modes is therefore a monotonic function of the quasimomentum k_x. Figure 3 shows the luminescence spectra in wires of width 4.2 μm, recorded at $\Theta = 18°$ for various angles Φ. The spectra were recorded at a high excitation density $P = 1600\ \text{W/cm}^2$, such that exciton–photon interaction is suppressed. At $\Phi = 0°$ two strong, narrow lines corresponding to modes $M1$ and $M2$ are visible in the spectrum against the background of the broad electron–hole recombination line. All other modes are seen as weak features in the spectrum. The mode energies at $\Phi = 0°$ are indicated by vertical arrows. As Φ increases, all the photon modes shift toward the violet end. The dashed curves in Fig. 3 represent the positions of modes $M0$, $M1$, and $M2$ as the angle Φ is varied. Particularly noticeable in the figure is the absence of anomalies in the behavior of the energies of the optical modes when they intersect the $e-h$ recombination peak. This behavior is characteristic of the suppression of interaction between light and carriers in quantum wells. The dispersion of photon modes $M0-M4$ is shown in Fig. 4. It is extracted from the luminescence spectra measured at $\Theta = 0°$ and 18° over a wide range of angles Φ. The large open circles indicate the energy of the $e-h$ recombination peak. As expected, its energy does not depend on the quasimomentum. Dark symbols represent the measured dispersion of the photon modes. The energy of mode $M3$ is shown only for $k_x < 10^3\ \text{cm}^{-1}$, because for large angles Φ this line has poor resolution against the background of the rather strong, broad $e-h$ recombination line. The solid curves represent the photon mode dispersion calculated

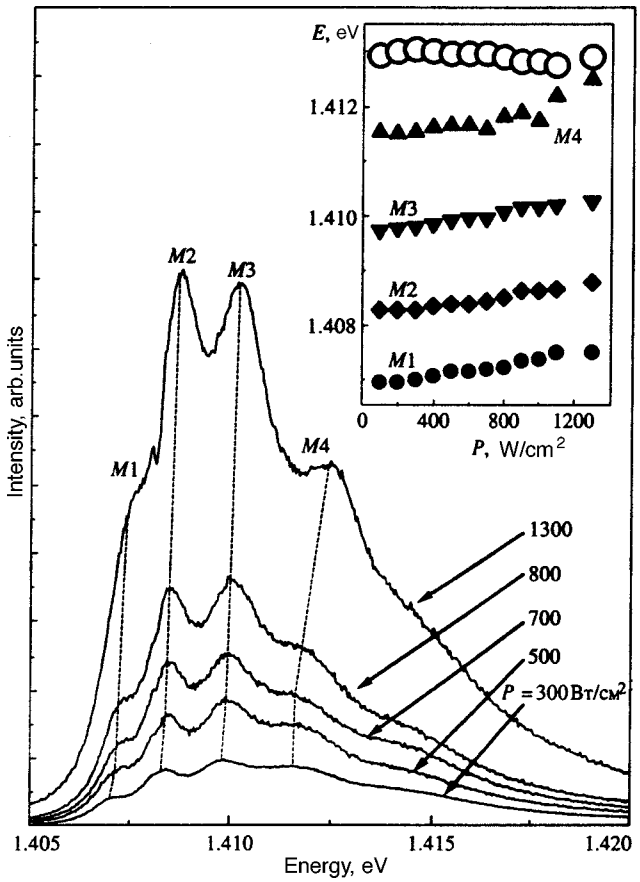

FIG. 5. Luminescence spectra of wires with $L_y = 6.2\ \mu$m, recorded for various excitation densities at $\Theta = 10°$ and $\Phi = 0°$. The dashed lines indicate the variation of the photon mode positions. Inset: energies of photon modes and the exciton peak (light circles) as functions of the excitation density.

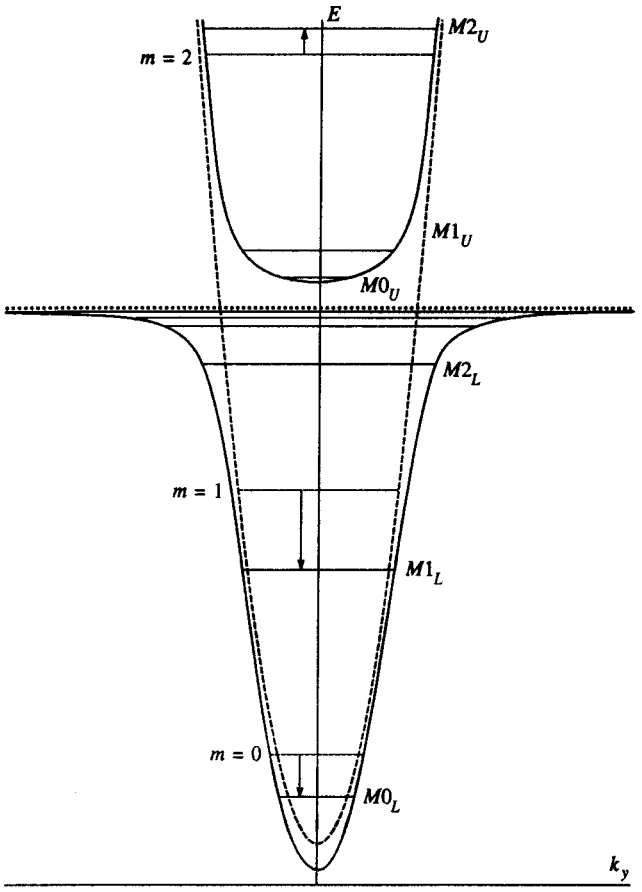

FIG. 6. Diagram of the quantization of polaritons in a photon wire (see the text).

from Eq. (3). The only fitting parameter used in the calculations is the dielectric permittivity. It is evident form the figure that the experimental curves are well described for $\varepsilon_{\text{eff}} = 10.9$. As expected, this value differs markedly from ε in the GaAs λ layer and is close to the average of the dielectric constants of AlAs (8.8) and GaAs (12.5). Indeed, owing to the low reflection coefficient at the boundary of the active layer, light penetrates the Bragg mirrors to a depth of several GaAs/AlAs layers.

4. VARIATION OF EXCITON–PHOTON INTERACTION AS THE DENSITY OF EXCITONS IS VARIED

Effects associated with exciton–photon interaction becomes more significant as the excitation density decreases. To illustrate the transition from the weak to the strong coupling regime, we refer to Fig. 5. It shows the luminescence spectra measured at $\Theta = 10°$ and $\Phi = 0°$ in wires of width 6.2 μm for various excitation densities. The angle $\Theta = 10°$ is chosen to achieve good resolution in the spectra simultaneously for all four optical modes $M1 - M4$, which are situated below the exciton energy of 1.413 eV. In Fig. 5 all four modes are seen as strong, narrow lines against the background of the weaker, broad exciton line. As the excitation density is decreased, all modes shift toward lower energies. The shifting of the peaks is reflected by the dashed curves in the figure. The inset to the figure shows the dependence of the mode energies on the excitation density.[2)] The repulsion of the cavity modes from the exciton term is evidence of the repulsion of exciton and photon states, i.e., strong coupling between excitons and photons in the microcavity.[3)] The most pronounced variation of the energy with decreasing excitation density is observed for $M4$, the mode closest to the excitation level. As the distance between the photon mode and the exciton peak increases, the degree of repulsion subsides considerably (from 1 meV for $M4$ to 0.5 meV for $M1$).

The experimental pattern of states in photon wires can be described in terms of quantized microcavity polaritons. The formation of polariton states in photon wires is illustrated in Fig. 6. We first consider a planar microcavity. If excitons and photons do not interact, they have a parabolic dispersion law. The dashed curve in Fig. 6 shows the photon dispersion, and the dashed curve represents the exciton energy level. The exciton energy depends weakly on k by virtue of the large effective exciton mass m_{ex} relative to the photon mass M_p: $m_{\text{ex}} \sim 10^5 M_p$ (Refs. 12 and 13). Exciton–photon interaction results in the production of a cavity polariton with a dispersion law described by the expression for two intersecting, interacting levels:[16]

$$E_{U,L}^2(k) = \frac{\Sigma^2 \pm \sqrt{\Sigma^4 - 4E_{\text{ex}}^2(k)E_p^2(k)}}{2}. \qquad (4)$$

Here $E_{U,L}(k)$ denotes the energies of the upper and lower branches of the polariton dispersion curve (with the plus or minus sign, respectively), $E_p(k)$ and $E_{\rm ex}(k)$ are the photon and exciton mode energies without interaction, $\Sigma^2 = E_{\rm ex}^2(k) + E_p^2(k) + \Omega^2$, and Ω is the splitting between the upper and lower branches at resonance. The dispersion of polaritons is represented by solid curves in Fig. 6. Far from resonance the lower branch of the polariton dispersion curve exhibits predominantly photon behavior for small k and predominantly exciton behavior for large k. The opposite pattern is encountered for the upper branch. For large k its dispersion is close to the dispersion of the photon mode without interaction. In a planar microcavity the dispersion of excitons, photons, and polaritons is independent of direction in the xy plane.

The confinement of light in the y direction by the semiconductor–vacuum boundaries (L_Y is of the order of a few μm) leads to quantization of the photon cavity mode. The lower quantized states ($m=0;1,2$) without exciton–photon interaction are represented by dashed horizontal lines in Fig. 6. The splitting of the exciton levels due to size quantization is very small and is therefore not shown in Fig. 6.

Polariton states corresponding to pair-interacting exciton and photon states with identical numbers m are formed in the strong exciton–photon coupling regime. In this case each m corresponds to two polariton states, one for the lower branch and one for the upper branch of the dispersion curve (solid horizontal lines labeled $Mm_{U,L}$) in Fig. 6.

It is evident from Fig. 6, consistent with experiment, that photon states situated below the exciton level ($m=0,1$ in the figure) are shifted downward on the energy scale (indicated by arrows in the figure). The shift decreases when the number m increases. Figure 6 shows that the more pronounced decrease of the energy level with $m=2$ is readily explained within the context of polariton quantization by an increase in the effective mass of the polaritons as the exciton level is approached. It is also evident from Fig. 6 that lateral quantization of the lower polariton branch in photon wires should produce a large number of levels in the vicinity of exciton resonance. These levels, in contrast with those with $m=0,1$, are excitonlike; the smallness of the splitting makes them spectrally unresolved.

We now consider the quantization of the upper polariton branch. It is evident from the figure that the energy of the polariton state $M2_U$, which is situated far from the exciton level, differs only slightly from the energy of the photon level with $m=2$ in the noninteracting system. The latter result is attributable to the large contribution of the photon component to this polariton state. States near the bottom of the upper polariton branch ($M0_U$, $M1_U$) are shifted slightly relative to the plateau as a result of the large polariton mass for small k. This behavior is explained by the large contribution of the exciton component to the polariton state. The smallness of the splitting makes it impossible to resolve states $M0_U$ and $M1_U$ in the luminescence spectrum for $k=0$, but it will be shown in the next section that they can be distinguished by analyzing the polariton behavior for large k_x.

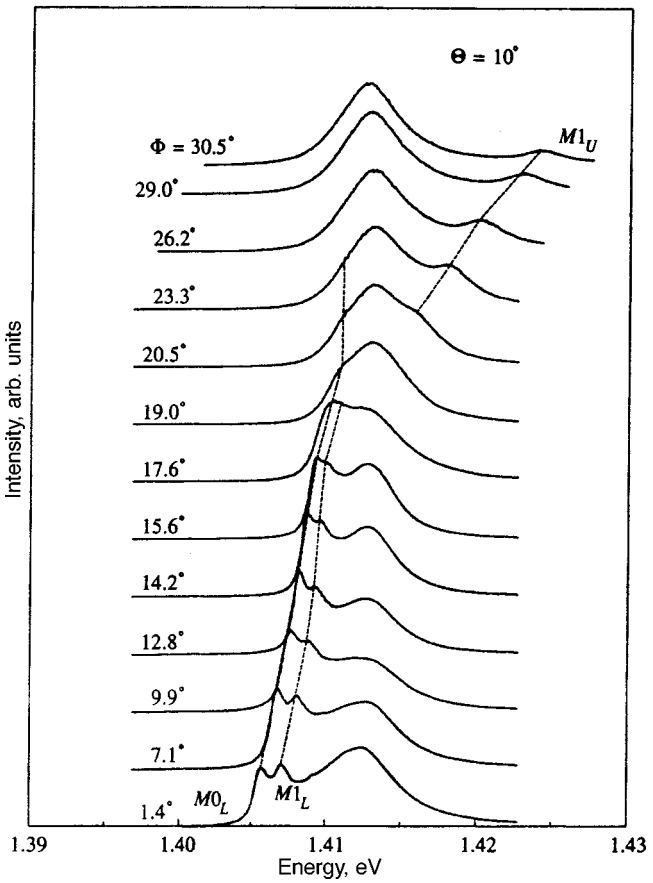

FIG. 7. Photoluminescence spectra for wires with $L_y = 4.2\ \mu$m, recorded at $\Theta = 10°$ and various angles Φ. The dashed lines indicate the positions of modes $M0$ and $M1$. The subscripts L and U signify the lower and upper branches of polariton dispersion.

5. DISPERSION OF POLARITONS IN PHOTON WIRES IN THE PRESENCE OF STRONG EXCITON–PHOTON COUPLING

To investigate the dispersion of polaritons in photon wires we have conducted a series of luminescence measurements at a low excitation density $P = 300\ \mathrm{W/cm^2}$ in wires of width 4.2 μm at various angles Φ. Since different mode orders are dominant in the spectra for different angles Θ, we carried out the series of measurements at three angles $\Theta = 0°, 10°, 15°$. One series is represented in Fig. 7, which shows luminescence spectra recorded at $\Theta = 10°$ and several angles Φ. As in the case of high excitation density, the photon modes shift toward higher energies as Φ increases. At low excitation densities, however, the photon modes go through an anticrossing with the exciton peak. This feature differs qualitatively from the high-density case (Fig. 4), which does not have any anomalies in the region of intersection of the photon modes and the exciton level. Moreover, it is evident from Fig. 7 that the branches of modes $M0$ and $M1$ situated below the exciton energy tend to the exciton level. For large Φ a new line appears above the exciton peak; it can be ascribed to the upper branch of the polariton mode $M1$. The exciton peak (1.413 eV) scarcely alters its position as Φ increases, but this is not too surprising in view of the major contribution of excitons in the regions between wires

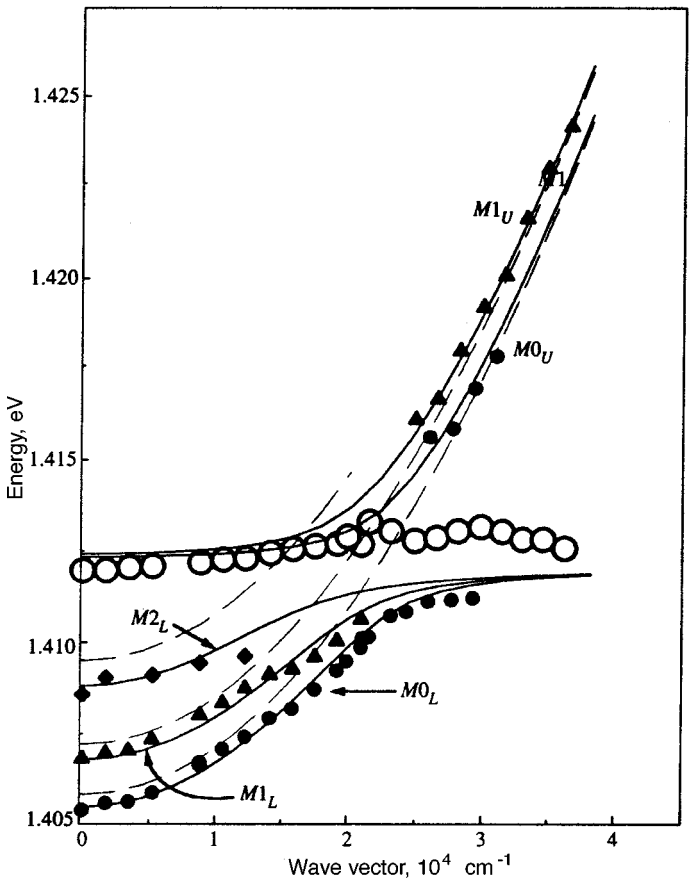

FIG. 8. Dispersion of polaritons in wires with $L_y = 4.2\ \mu$m, obtained from the luminescence spectra for a low excitation density. The subscripts L and U signify the lower and upper branches of polariton dispersion. Dark symbols represent the polariton mode energies. The solid curves are calculated from Eq. (4). The dashed curves represent the photon mode dispersion determined from measurements at a high excitation density.

to the luminescence signal. The formation of the polariton modes $M0_U$, $M0_L$, and $M2_L$ is also observed in the other series of measurements at $\Theta = 0°$ and 15°.

The observed anticrossing of exciton and photon states indicates the formation of microcavity polaritons. The polariton mode dispersion determined from an analysis of the energies of the spectral peaks in Fig. 7 is shown in Fig. 8. The corresponding mode energies measured at high excitation density, when the interaction of light with excitons is suppressed, are also shown (dashed curves) for comparison. A comparison of the mode energies at low and high excitation densities shows that exciton–photon mixing has the effect of shifting cavity modes with $E < E_{\rm ex}$ toward lower energies and shifting modes with $E > E_{\rm ex}$ toward higher energies. This behavior is natural when each mode interacts with the exciton state corresponding to it in terms of spatial symmetry. Consequently, to describe the experimental results for each pair $E_{mU,L}(k)$ we have used Eq. (4), replacing $E_p(k)$, $E_{\rm ex}(k)$, and Ω by their counterparts for the given mth mode: $E_m(k_x)$, $E_{{\rm ex},m}(k_x)$, and Ω_m. We obtain the photon mode energies $E_m(k_x)$ from the spectra at high energy density. We then disregard the exciton quantization energies, i.e., we assume that $E_{{\rm ex},m} = E_{\rm ex} = 1.413$ eV for all $m = 0, 1, 2$. For low mode orders m ($m = 0-2$) the splitting Ω_m in wide photon wires should not depend too strongly on the photon mode order, i.e., we can set $\Omega_0 = \Omega_1 = \Omega_2 = \Omega$. We are thus left with only the one fitting parameter Ω to describe several polariton branches in Eq. (4). Better agreement between the calculated curves and the experimental points is attained for $\Omega = 3$ meV. The corresponding fitted curves are shown as solid curves in Fig. 8. The magnitude of the interaction in the case of photon wires is found to be slightly lower than in the original planar microcavity. It has been determined from similar measurements of the luminescence spectra in a planar microcavity that $\Omega = 4$ meV. The reduction of Ω in wires is most likely attributable to lowering of the Q of the structure in etching of the planar microcavity.

The better agreement of the experimental polariton dispersion curves with those calculated on the assumption of interaction between exciton and photon states of like spatial symmetry indicates that exciton–photon interaction retains essentially the same character as in a microcavity with an ideal quantum well, despite the fact that potential fluctuations in a real quantum well lead to the localization of excitons and induce breaking of the symmetry of their states. In the structures we studied the localization range for excitons in a quantum well does not exceed $0.1-0.2\ \mu$m, whereas L_y is an order of magnitude higher: $4-6\ \mu$m. To explain the weak influence of a random potential for the indicated ratio of the characteristic dimensions, it must be assumed that in a photon wire an optical mode induces a collective coherent state of excitons of like symmetry. This state is constructed from a large number of localized and free exciton states. The interaction of light with such exciton modes results in the formation of coherent polariton states. This kind of interaction mechanism is possible by virtue of the fact that the light wavelength is much greater than the exciton radius, so that a great many exciton states are excited coherently at the same

time. It is obvious that the coherent state has a finite lifetime, owing to the scattering of excitons by the random potential and phonons and because of exciton–exciton collisions. The polariton dispersion observed by us in photon wires indicates that the dephasing time of polariton states is at least greater than the Rabi oscillation period (~ 0.4 ps). This conclusion is consistent with a measurement of the dephasing time of exciton states by the four-wave mixing method,[17], where a dephasing time of 12 ps has been determined for a low-density exciton system. The dephasing time decreases as the exciton density increases, accounting for our experimentally observed suppression of exciton–photon interaction at high excitation densities.

6. CONCLUSION

In 2D optically confined semiconductor microcavities we have investigated the structure of the states of the phonon system and the dispersion of cavity polaritons in the presence of strong exciton–photon coupling. Light is spatially confined in one dimension by a system of Bragg mirrors and in the other dimension by the semiconductor–vacuum boundary. The lateral confinement of the cavity leads to quantization of the vertical cavity mode. The additional photon states have a maximum in the luminescence spectrum at various values of the angle Θ. At low excitation densities exciton–photon coupling is fairly strong and results in the formation of cavity polaritons. The experimental polariton dispersion curves are in good agreement those calculated on the assumption that interaction takes place only between photon and exciton states of like spatial symmetry. Fluctuations of the random potential in the quantum wells break the spatial symmetry of the excitons but have little influence on the dispersion of polaritons. Consequently, polaritons are produced in microcavities through collective coherent exciton states induced by the optical electromagnetic field. The dephasing time of such states is much longer than the Rabi oscillation period. As the excitation density increases, the screening of exciton states and shortening of the dephasing time have the effect of suppressing the strong exciton–photon coupling regime.

We are grateful to M. Bayer, R. Sirus, S. Tikhodeev, N. Gippius, and A. Dzyubenko for profitable discussions and also to the International Association for the Promotion of Cooperation with Scientists from the Independent States of the Former Soviet Union (INTAS), the Russian Fund for Fundamental Research, and the ''Physics of Solid State Nanostructures'' Program for financial support.

*)E-mail: tarta@issp.ac.ru
†)E-mail: kulakovs@issp.ac.ru

1)In reality, the boundary conditions on the side walls of the cavity differ for excitons and light, so that orthogonality is lost between the wave functions of exciton and photon modes having different orders. As a consequence, the interaction of even (odd) exciton modes with all even (odd) photon modes is allowed. However, interaction between modes of like orders must be dominant.

2)The photon mode energies and the position of the exciton recombination peak, which is not resolved as a distinct band in the spectra of Fig. 5, have been determined by the application of a program for deconvolution of the spectral positions of peaks by fitting of the line shape.

3)The position of the exciton peak does not change, because the main contribution to the exciton luminescence signal is from excitons that recombine in the region between the wires. In fact, the dimensions of these regions exceeds the area of the photon wires, and the essentially completely etched Bragg mirrors are two or three orders of magnitude more transparent both to the exciting laser beam and to exciton radiation. It is obvious that exciton–photon interaction is not intensified by the cavity in the regions between wires, and the position of the exciton peak therefore remains unchanged in transition from the weak to the strong exciton–photon coupling regime.

[1] V. Savona, L. C. Andreane, P. Schwendimann, and A. Quattropani, Solid State Commun. **93**, 733 (1995).
[2] V. Savona and F. Tassone, Solid State Commun. **95**, 733 (1995).
[3] V. Savona, Z. Hradil, A. Quattropani, and P. Schwendimann, Phys. Rev. B **49**, 8774 (1994).
[4] S. Jorda, Phys. Rev. B **50**, 18690 (1994).
[5] S. Jorda, Phys. Rev. B **51**, 10185 (1995).
[6] R. Houdré, R. P. Stanley, U. Oesterle, M. Ilegems, and C. Weisbuch, Phys. Rev. B **49**, 16761 (1994).
[7] R. Houdré, C. Weisbuch, R. P. Stanley *et al.*, Phys. Rev. Lett. **73**, 2043 (1994).
[8] R. Houdré, J. L. Gibernon, P. Pelladini *et al.*, Phys. Rev. B **52**, 7810 (1995).
[9] J. P. Reithmaier, M. Rohner, H. Zull *et al.*, Phys. Rev. Lett. **78**, 378 (1997).
[10] B. Ohnesorge, M. Bayer, A. Forchel *et al.*, Phys. Rev. B **56**, 4367 (1997).
[11] R. Houdré, R. P. Stanley, and M. Ilegems, Phys. Rev. A **53**, 2711 (1996).
[12] D. M. Whittaker, P. Kinsler, T. A. Fisher *et al.*, Phys. Rev. Lett. **77**, 4792 (1996).
[13] V. Savona, C. Piermarochhi, A. Quattropani *et al.*, Phys. Rev. Lett. **78**, 4470 (1997).
[14] T. B. Borzenko, Y. I. Koval, L. V. Kulik, and V. V. Larionov, Appl. Phys. Lett. **70**, 2297 (1997).
[15] N. A. Gippius, S. G. Tikhodeev, and A. Forchel, in *Digests of the Third All-Russian Conference on the Physics of Semiconductors* [in Russian] (FIAN, Moscow, 1997).
[16] B. Sermage, S. Long, I. Abram *et al.*, Phys. Rev. B **53**, 16516 (1996).
[17] A. Honold, L. Schultheis, J. Kuhl, and C. W. Tu, Phys. Rev. B **40**, 6442 (1989).

Translated by James S. Wood